ISSN (Print) 1226-1750
ISSN (Online) 2233-6656
Journal of Magnetics 24(2), 303-309 (2019) https://doi.org/10.4283/JMAG.2019.24.2.303

Comparison of the SPIR and STIR MR Pulse Sequences in an Oil and Water Phantom

Song Yoon Lee, Jin Han, and Dae Cheol Kweon*

Department of Radiological Science, College of Bioecological Health, Shinhan University, Uijeongbu 11644, Republic of Korea

(Received 8 February 2019, Received in final form 11 April 2019, Accepted 11 April 2019)

The coexistence of fat and water in the human body causes difficulties in obtaining accurate images using magnetic resonance imaging (MRI). This study evaluated the usefulness of the spectral pre-saturation inversion recovery (SPIR) and short TI inversion recovery (STIR) pulse sequences in suppressing fat. MRI of a water-oil phantom was performed using an Ingenia 3.0-T scanner (Philips Medical Systems, Best, The Netherlands). For quantitative evaluation of the images, the plot profile, signal-to-noise ratio (SNR), and contrast-to-noise ratio (CNR) were measured and compared using ImageJ program (NIH, Bethesda, MD, USA). The SNR for water was higher by 56.04 % on STIR (403.59) than on SPIR (258.64). The SNR for fat was higher by 52.10 % on STIR (17.34) than on SPIR (11.40). The CNR was higher by 24.87 % on STIR (308.75) than on SPIR (247.24). Compared to SPIR, the STIR pulse sequence showed a better fat clearing effect. Therefore, it is necessary to select the appropriate fat suppression method according to the clinical necessity.

Keywords : Chemical shift, CNR, Fat suppression, MRI, Phantom, SNR, SPIR, STIR

1. Introduction

Magnetic resonance imaging (MRI) is an imaging approach for living body tissues that is based on the fact that the magnetic resonance phenomenon of hydrogen nuclei differs between tissues of the human body [1]. MRI is a technique to image signals generated by tissue using the resonance phenomenon and does not harm the human body because it uses non-ionizing radiation. Using powerful magnetic fields and radio waves, images of body structures, such as soft tissues and bones, can be obtained. However, it is somewhat difficult to obtain accurate images using MRI because of the presence of fat and water components in living tissue. Fat and water induce T1 and T2 relaxation time differences and artifacts due to inadequate contrast or chemical shift in conventional MRI techniques due to the sensitivity of the magnetic resonance imaging signal [2]. Specifically, due to the different chemical environments, hydrogen nuclei in water and adipose tissues differ in their values, primarily chemical relaxation time and resonance frequency chemical shift, for some MRI parameters. These differences can be used to selectively inhibit or reduce the signal of lipoprotein protons [3].

Local erasure is useful in terms of selective signal acquisition but, if not properly used when necessary, has the following problems. Small amounts of fat are more difficult to detect on conventional MRI. Moreover, due to the high signal due to fat, artifacts such as ghosting and chemical migration can occur. Furthermore, high signals can mask subtle differences in non-fat tissue by filling the receiver's dynamic range primarily with fat signals. Finally, contrast-enhanced tumors may be hidden by surrounding fat [4]. Therefore, it is necessary to suppress the fat signal to obtain more accurate image information.

Various pulse sequences are used to suppress fat, but in this study, we focused on the following two methods. First, the spectral pre-saturation inversion recovery (SPIR) technique selectively suppresses the signal from adipose tissue by applying a high frequency pulse equal to the resonance frequency of the adipose tissue in a chemical saturation method using a specific frequency. This technique has advantages in that it can be used with any imaging technique because it applies the selective high frequency pulse to the proton selection high frequency, using the difference in the proton resonance frequency of the adipose tissue and water molecules; it is therefore suitable for inhibiting tissue. In the short TI inversion

*Corresponding author: Tel: +82-31-870-3411
Fax: +82-31-870-3419, e-mail: dckweon@shinhan.ac.kr

recovery (STIR) technique, fat suppression is based on tissue relaxation time. The 180° pulse first reverses the longitudinal magnetization, and the fat signal passes through the null point precisely (0.69 × TI) to start image acquisition. STIR is not sensitive to the non-uniformity of the magnetic field and can be used in low magnetic fields [5]. It is important to consider the quality of images by comparing the best techniques currently available for fat suppression. This technique of fat suppression technique is applied to the abdomen and various organs in the clinic and MRI scanned for diagnosis [6, 7].

In this study, we quantitatively evaluated and compared the SPIR and STIR pulse sequences and assessed the usefulness and applicability of these techniques in fat suppression in clinical practice.

2. Fat Suppression Techniques

Fat suppression techniques are used in generic term that includes various techniques of chemical shift selective (CHESS), STIR, and SPIR the features of these techniques are advantages, disadvantages and pitfalls [4]. Fat suppression techniques can be applied to both T1- and T2-enhanced pulse sequences commonly used in MRI to suppress signals from adipose tissue or to detect adipose tissue. Due to the short relaxation time, fat has a high signal on MRI. This high signal, which can be easily recognized on MRI, can be useful for characterizing lesions [5]. The optimal fat suppression technique of MR pulse sequence depends on the amount of fat needed to suppress the MR signal intensity. We describe below the key features of CHESS, STIR and SPIR in fat suppression MR pulse sequence. The CHESS method was developed by Haase *et al.* This technique selectively images only fat or water using the chemical shift effect. It can be used as a technique to suppress water or obtain an image by suppressing fat [8].

2.1. Spectral Pre-saturation Inversion Recovery

The excitation RF pulse is then applied when the fat signal is zero-crossing during T1 recovery [4] (Fig. 1a). SPIR is a hybrid technique of STIR and the CHESS pulse method, a commonly used fat suppression technique; that is, the inversion radiofrequency (RF) pulse of STIR is replaced with the CHESS pulse, and only the fat component is inverted (Fig. 1b).

2.2. Short TI Inversion Recovery

The STIR pulse sequence applies an inversion pulse and time delay (TI) into the range of the time inversion values from the lipomatous of soft tissue (Fig. 2). Based on an inversion recovery pulse sequence, the 180° μRF pulse first inverts the longitudinal magnetization and

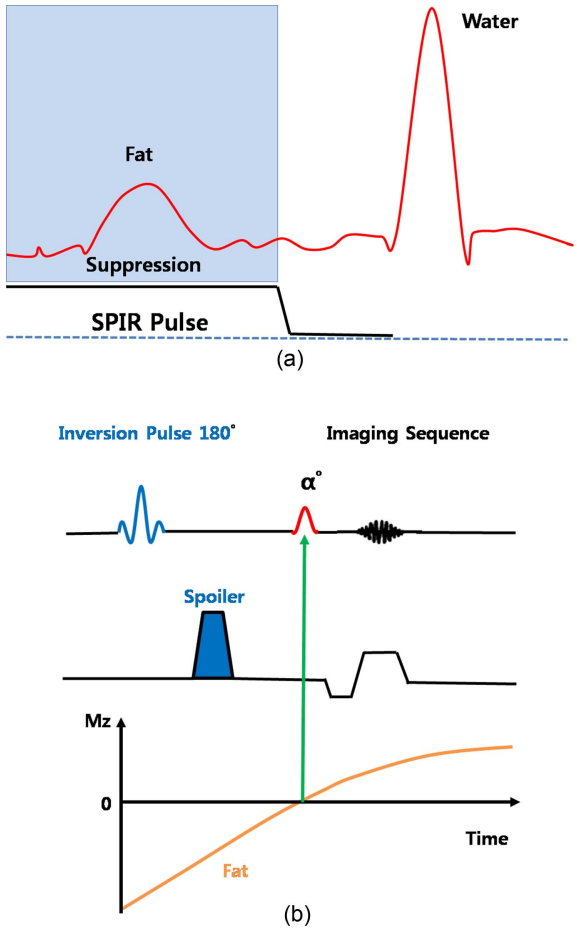

Fig. 1. (Color online) SPIR pulse sequence diagram for fat suppression (a). SPIR pulse sequence hybrid features of CHESS and STIR (b).

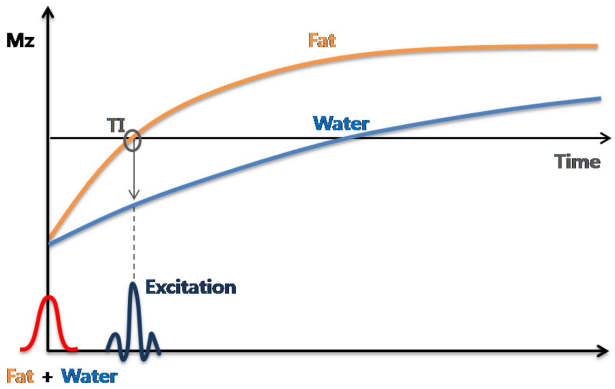

Fig. 2. (Color online) STIR pulse diagram for fat suppression and signal intensity with inversion recovery imaging. Diagram shows the behavior fat tissue signal and water signal during the inversion recovery sequence and how tissue with a short TI (fat) and tissue with a long TI (water) may produce the same signal intensity.

Table 1. Magnetic resonance imaging scanning parameters used in the SPIR and STIR pulse sequences.

Parameter	SPIR	STIR
FOV (mm)	160 × 160 × 165	160 × 160 × 165
Voxel (mm)	0.5 × 0.62 × 3	0.7 × 0.71 × 3
Matrix (slice)	320 × 256 × 50	228 × 217 × 50
TR (ms)	4466	8237
TE (ms)	80	60
TI (ms)		200
Flip angle (°)	90	120
NSA	1	1

FOV: field of view, TE: echo time, TI: inversion time, TR: repetition time, NSA: number of signals averaged, SPIR: spectral pre-saturation inversion recovery, STIR: short TI inversion recovery

waits for the TI time to recover; that is, when a 180° RF pulse is applied, the magnetization component in the vertical axis direction is formed on the negative z-axis. When the RF pulse is discontinued, the RF pulse relaxes on the positive z-axis and reaches a null point. The tissue does not produce a signal, and only the signals of other tissues are detected in the image signal [9, 10].

3. Materials and Methods

3.1. Phantom Experiments

A phantom using water and canola oil (Dongwon Co., Ltd, Seoul Korea) as a human equivalent material with different chemical environments was fabricated and tested. The bottle was filled with 250 cm^3 of water and canola oil, and the bubble was removed to clarify the boundary between water and oil. MRI was performed using an Ingenia 3.0-T scanner (Philips Medical Systems, Best, The Netherlands). The SPIR and STIR sequences were used, and the scan parameters are shown in Table 1 (Fig. 3).

3.2. Analysis of MR Imaging

Image analysis was performed using ImageJ (NIH, Bethesda, MD, USA) and the plot profile was obtained to evaluate image quality. The signal-to-noise ratio (SNR) and contrast-to-noise ratio (CNR) were calculated and used as indices of image quality. In the collected images, a 15 × 15-mm region of interest was identified to measure the water, and the fat signal intensity (SI) in the phantom was measured. The background SI was measured at the outer upper part of the phantom (Fig. 4).

The SNR was calculated by dividing the signal strength of the central part of the water or fat by the background SI as shown in Equation (1).

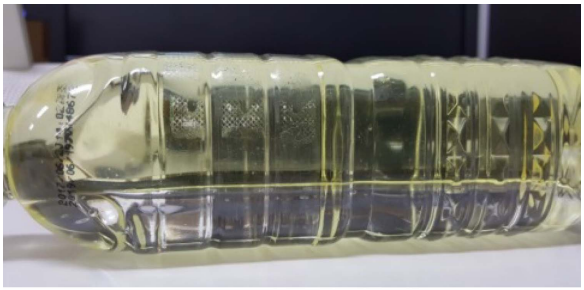

(a)

(b)

Fig. 3. (Color online) Water-oil phantom (a) and magnetic resonance imaging equipment (b).

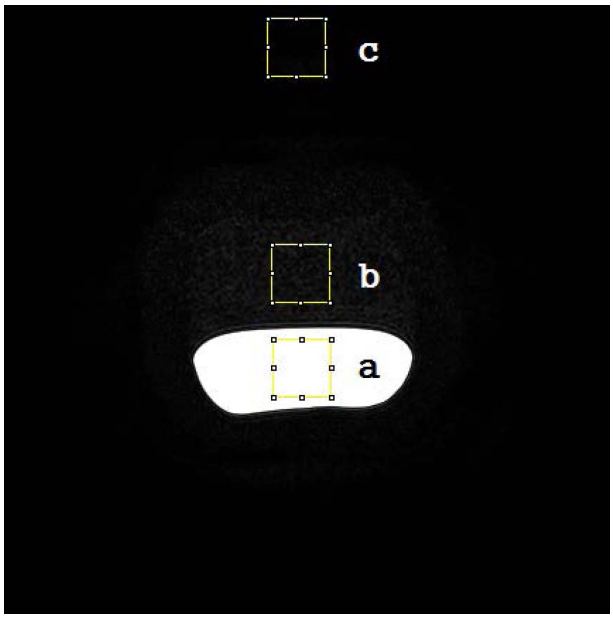

Fig. 4. (Color online) Region-of-interest (ROI) located in water (a). ROI located in fat (b). ROI located in the background (c).

$$\text{SNR} = \frac{\text{SI}}{\text{Background SI}} \quad (1)$$

The CNR was calculated by dividing the difference between the central signal strength of the water and central SI of the fat by the background SI as shown in Equation (2):

$$\text{CNR} = \frac{\text{Water SI} - \text{Fat SI}}{\text{Background SI}} \quad (2)$$

3.3. Statistical Analysis

Statistical analysis was performed using SPSS 21.0 (IBM Corp., Armonk, NY, USA). SPIR and STIR were compared using independent t-tests. The differences in the quantitative analysis were statistically significant when the *p*-value was lower than 0.05.

4. Results

The selected MR scanning images to perform the oil and water phantom were most consistent with the proposed goal according to the STIR and SPIR pulse sequences.

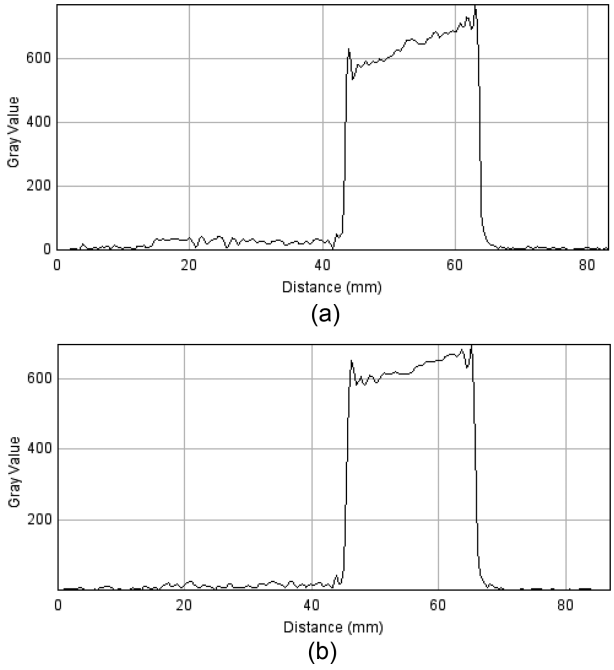

Fig. 5. Plot profile of the SPIR pulse sequence (a) and STIR pulse sequence (b) of gray value and distance using the water-oil phantom.

Table 2. SNR for the SPIR and STIR pulse sequences.

		SPIR	STIR	p-value
SNR (Mean ± SD)	Water	253.1 ± 7.71	407.401 ± 7.75	< 0.05
	Fat	11.068 ± 0.37	17.22 ± 0.39	< 0.05

SNR: signal-to-noise ratio, SPIR: spectral pre-saturation inversion recovery, STIR: short TI inversion recovery

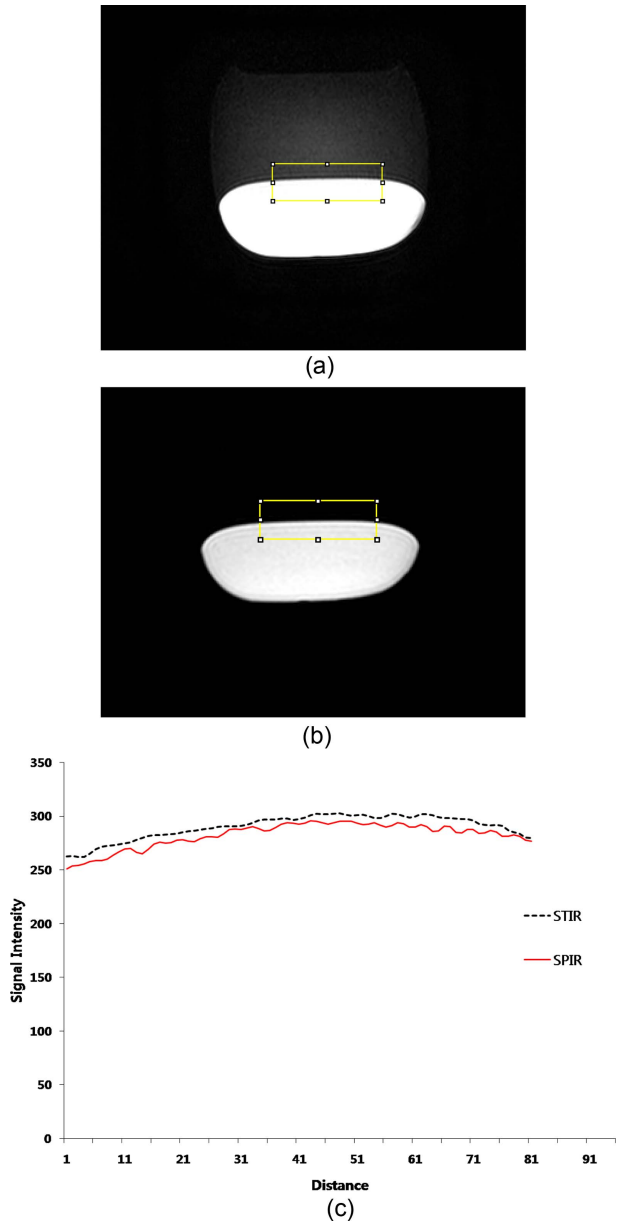

Fig. 6. (Color online) Rectangular ROI measured of SPIR (a) and STIR pulse sequence (b). Signal intensity of plot profile of barrier of water and oil phantom (c).

The plot profile according to the MR sequence is shown in Fig. 5. At the same distance, the profile of the water was drawn more gently on STIR than on SPIR. The local profile showed further suppression in STIR. The SNR values of water and fat in the MR sequence are shown in Table 2. The SNR for water was 258.64 on SPIR and 56.04 % higher, at 403.59, on STIR. The SNR for fat was 52.10 % higher for STIR (17.34) than for SPIR (11.40). The SNR values on STIR were higher than they were on SPIR for both water and fat.

Rectangular ROIs measured of barrier an oil and water

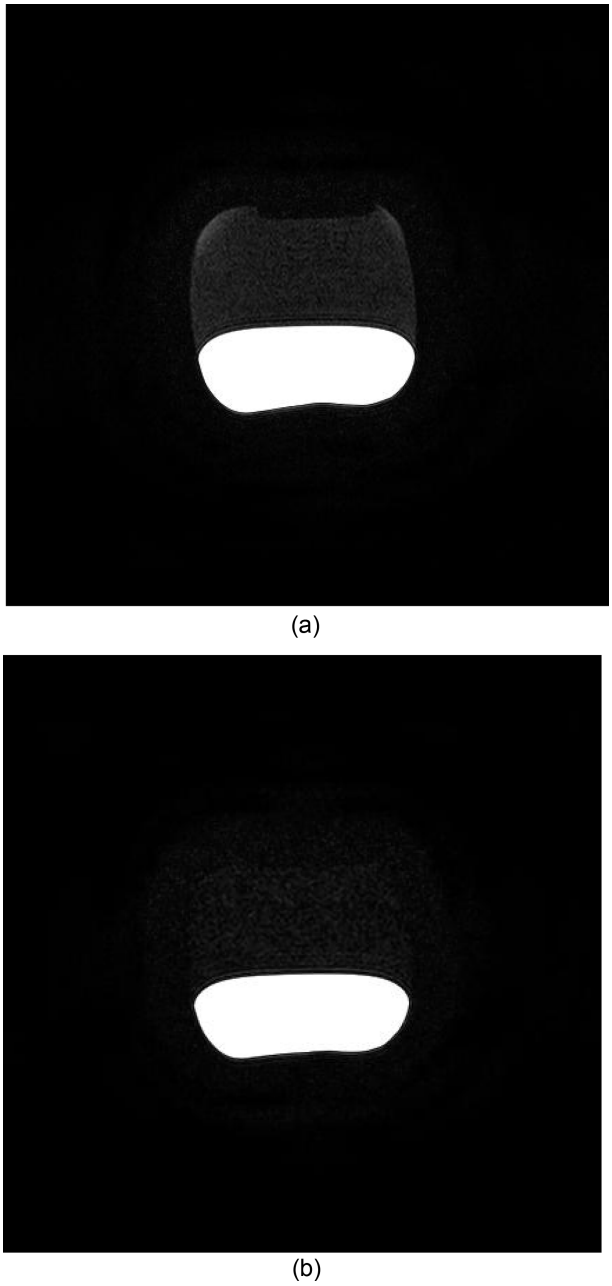

Fig. 7. Fat suppression in SPIR (a) and STIR pulse sequences (b).

phantom (Fig. 6a, b) and signal intensity data displays of STIR and SPIR pulse sequence MR image. In Fig. 6c, the STIR pulse sequence was measured higher than the SPIR at the signal intensity measured using the function of the plot profile.

The image according to each pulse sequence is shown in Fig. 7. Table 3 shows the measured CNR values according to the pulse sequence. The CNR on STIR (308.75) was 24.87 % higher than that on SPIR (247.24). In all comparisons of the STIR and SPIR pulse sequences,

Table 3. CNR for the SPIR and STIR pulse sequences.

	SPIR	STIR	p-value
CNR (Mean ± SD)	242.028 ± 7.35	390.17 ± 7.47	< 0.05

CNR: contrast-to-noise ratio, SPIR: spectral pre-saturation inversion recovery, STIR: short TI inversion recovery

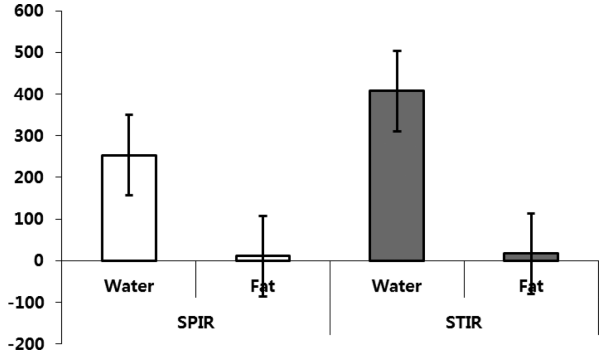

Fig. 8. SNR of fat and water data presented as mean and standard deviation. The *p*-value was determined using an unpaired t-test.

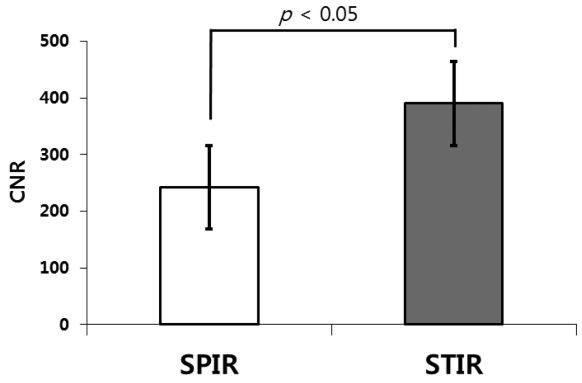

Fig. 9. CNR data presented as mean and standard deviation. The *p*-value was determined using an unpaired t-test.

the *p*-value was lower than 0.05 (Fig. 8, Fig. 9).

5. Discussion

MRI shows chemical migration phenomena between water and fat. Fat has a strong signal that can form false artifacts. In order to provide diagnostic information for the human body, fat suppression techniques are indispensable, and methods for obtaining images with fat suppression include the CHESS, SPIR, and STIR pulse sequences [11, 12]. In addition, when comparing the existing STIR, SPIR, and spectral attenuated inversion recovery (SPAIR) MR pulse sequences, it has been confirmed to be advantage in MR examinations of breast patients [13, 14]. In the 3.0-T diffusion weighted imaging

(DWI) images based on STIR and SPAIR were suitable for identifying and characterizing breast lesions [15].

In this study, the SPIR and STIR fat suppression techniques were compared, and an experiment was conducted to evaluate their usefulness. We observed a difference between the two sequences of SPIR and STIR pulse sequences. SPIR is a combination of the CHESS, which is typically used, and STIR techniques. The fat signal is inverted by the inversion RF pulse of STIR and becomes null. When the point reaches 0, an excitation RF pulse is applied to suppress fat [12]. It is mainly used for T1- and T2-weighted image fat suppression in regions not containing a metal component using a spin echo pulse sequence. The oblique magnetic field echo is a phenomenon in which a metal component is not included in the test site and is mainly used for fat suppression in the test [16].

STIR is a fat suppression technique in which a 180° reversal pulse is applied before the 90° RF of the spin-echo technique to invert the longitudinal axis magnetization and is followed by TI to start image acquisition. TI depends on the component to be inhibited and the strength of the magnetic field. At 1.5-T, the TI of the fat component is 150-175 ms. The STIR technique is not sensitive to magnetic field heterogeneity, homogeneously inhibits adipose tissue, and enhances the clarity of the lesion by increasing the T1 and T2 contrasts [17]. However, existing studies that examined various local suppression techniques did not achieve the same results. The results show that the turbo-spin-echo (TSE)-SPIR fat suppression technique is superior to the gradient echo-principle of selective excitation technique (GE-PROSET) fat suppression technique in T2-weighted fat suppression neurologic and abdominal MRI examination because fat suppression was generally good [18, 19].

In addition, a comparison between TSE-CHESS and TSE-SPAIR showed that TSE-SPAIR is superior to the fat suppression technique in quantitative image analysis and statistical analysis [16, 20]. In a study evaluating the usefulness of STIR images in breast MRI, the results of the statistical comparison showed that the water and fat findings of lesions in fibrotic or fatty breast tissue were superior to those of T1- and T2-weighted STIR images [21]. In addition, there was no statistically significant difference in fat suppression between the STIR and SPAIR pulse sequences; however, the image quality obtained SPAIR was statistically significantly better than that obtained with STIR [22]. The results of this study showed that STIR was superior to lipid signal suppression in the lumbar spine, hip, and knee joint, and that SPAIR had superior image quality [23, 24].

Other studies have reported findings similar to ours. In addition to studies evaluating the usefulness of various fat suppression techniques, this study provided basic data enabling the optimal selection of a fat suppression technique through the comparison of the STIR and SPIR techniques.

The limitation of this study was that a water and oil phantom was used to perform the experiment to examine the chemical composition of fat and water alone, without consideration of the various other components of the human body. The problem with the study is that the patient is not available due to ethical procedures. Also, there are no related articles to guide us because there are no similar research yet [14]. Therefore, it is necessary to apply it to clinical practice in the future. Our view of the benefits of this study was an MRI experiment using a water and oil phantom.

6. Conclusion

The suppression of fat signals from oil and water phantom is inconsistent and non-uniform component. The radiological technologist has access to a variety of fat suppression techniques that operate using specific properties of MR signals of fat and water. In this research, the obtained results by the STIR and SPIR pulse sequence. Higher CNR and SNR can be attained using the STIR pulse sequence compared to the SPIR sequence, and the fat suppression effect can be confirmed in images. Therefore, STIR is more effective than SPIR for fat suppression. However, the radiological diagnosis is likely to be based on the need for appropriate fat suppression techniques.

References

[1] R. Ross, B. Goodpaster, D. Kelley, and F. Boada, Ann. N. Y. Acad. Sci. **904**, 12 (2000).
[2] H. H. Houchun and S. N. Krishna, Magn. Reson. Med. **63**, 494 (2010).
[3] W. Horger, Fat suppression in the abdomen, Magnetom Flash, Siemens Medical Solution, Erlangen, Germany. **3**, 114 (2007).
[4] E. M. Delfaut, J. Beltran, G. Johnson, J. Rousseau, X. Marchandise, and A. Cotton, Radiographics **19**, 373 (1999).
[5] T. A. Bley, O. Wieben, C. J. François, J. H. Brittain, and S. B. Reeder, J. Magn. Reson. Imaging. **31**, 4 (2010).
[6] K. Tanabe, K. Nishikawa, T. Sano, O. Sakai, and H. Jara, J. Magn. Reson. Imaging. **31**, 12777 (2010).
[7] S. S. Pokharel, K. J. Macura, I. R. Kamel, and A. Zaheer, Radiographics. **33**, 681 (2013).
[8] A. Haase, J. Frahm, W. Hänicke, and D. Matthaei, Phys.

Med. Biol. **30**, 341 (1985).
[9] A. S. Gaspar, R. G. Nunes, G. Ferrazzi, E. J. Hughes, J. Hutter, S. J. Malik, L. McCabe, K. P. Baruteau, M. A. Rutherford, J. V. Hajnal, and A. N. Price, Magn. Reson. Med. **81**, 477 (2019).
[10] F. Del Grande, F. Santini, D. A. Herzka, M. R. Aro, C. W. Dean, G. E. Gold, and J. A. Carrino, Radiographics **34**, 217 (2014).
[11] E. H. Koo, J. Digit. Pol. Management. **11**, 599 (2013).
[12] E. H. Koo, J. Korea Acad. Industr. Coop. Soc. **14**, 4962 (2013).
[13] H. Kato, M. Kuroda, K. Yoshimura, A. Yoshida, K. Hanamoto, S. Kawasaki, K. Shibuya, and S. Kanazawa, Med. Phys. **32**, 3199 (2005).
[14] M. M. Ribeiro, L. Rumor, M. Oliveira, J. G. O'Neill, and J. C. Maurício, J. Biomed. Sci. Eng. **6**, 395 (2013).
[15] S. Brandão, L. Nogueira, E. Matos, R. G. Nunes, H. A. Ferreira, J. Loureiro, and I. Ramos, Radiol. Med. **120**, 705 (2015).
[16] E. H. Koo, J. Digit. Pol. Management. **11**, 529 (2013).
[17] S. H. Kook, J. Korean Radiol. Soc. **49**, 427 (2003).
[18] A. S. Borthne, J. B. Dormagen, K. I. Gjesdal, T. Storaas, I. Lygren, and J. T. Geitung, Eur. Radiol. **13**, 100 (2003).
[19] S. W. Kim, C. H. Kim, M. S. Kim, Y. J. Jung, and W. M. Byun, J. Korean Neurosurg. Soc. **54**, 30 (2013).
[20] K. E. Cho, C. S. Yoon, H. T. Song, Y. H. Lee, D. Lim, J. S. Suh, and S. Kim, J. Korean Soc. Magn. Reson. Med. **17**, 110 (2013).
[21] H. M. Lee, J. Radiol. Sci. Technol. **32**, 95 (2009).
[22] H. J. Kang, S. H. Kook, Y. R. Lee, M. H. Lee, H. W. Par, W. J. Moon, S. K. Kim, and E. C. Chung, J. Korean Radiol. Soc. **49**, 427 (2003).
[23] H. M. Lee, J. Radiol. Sci. Technol. **33**, 45 (2010).
[24] H. M. Lee, H. G. Kim, and S. K. Kong, J. Radiol. Sci. Technol. **32**, 95 (2009).